

MEMS-Based Microfluidic Fuel Cell for In Situ Analysis of the Cell Performance on The Electrode Surface

Yusuf Dewantoro Herlambang¹, Anis Roihatin¹, Kurnianingsih², Shun- Ching Lee³, Jin-Cherng Shyu^{3*}

¹Department of Mechanical Engineering, Politeknik Negeri Semarang, Indonesia

²Department of Electrical Engineering, Politeknik Negeri Semarang, Indonesia

³Department of Mechanical Engineering, National Kaohsiung University of Science and Technology, Taiwan

*Corresponding author email : jcshyu@nkust.edu.tw

Abstract. The present study investigates various effects of MEMS-based microfluidic fuel cell on the performance of direct formic acid microfluidic fuel cells that breathe air as an oxidant. A miniaturized fuel cell of the structure and design of a typical T-shaped air-breathing Direct Formic Acid Fuel Cell with micro channel is 1.5 mm x 25 mm in width multiply length. Both anode and cathode electrode having a width and length of 0.6 mm and 20 mm, respectively, with an electrode spacing of 0.3 mm. An air-breathing microfluidic fuel cell having a 0.6 mm in width and 20 mm in length that is placed on cathode GDE down-side. In such systems for the fluid delivery, both formic acid (0.5 M) as a fuel solution mixing sulfuric acid (0.5 M) at a node channel side and as an electrolyte used sulfuric acid (0.5 M) place take on the cathode channel side are injected together into the end of the channel outlet by two syringe pumps. Firstly, a three-dimensional microfluidic fuel cell model was established using Computational Fluids Dynamics to simulate the fuel cell performance. Further, both V-I curves obtained from simulation and published experimental data under similar operating condition were compared to assure the validity of the simulation. Modelling the transport and electrochemical phenomena were described with hydrodynamic equations, the porous media flow, mass transport, electrochemical reaction and charge equation. The porous media flow in the gas diffusion layer was described by Brinkman equation. The Butler-Volmer equations were applied to get the V-I-P curves. An anode electrode surface performance, respectively, is presented.

1. Introduction

In recent years, the power generation for small power applications has been growing rapidly along with the begin abandonment of conventional power plants based on fossil fuels. Many renewable energy sources are used as micro-scale power generation which can be mass-produced with a micro-scale miniaturization technology [1, 2]. An application of micro-scale renewable energy generation has increased very significantly. In particular, micro portable devices that can be operated continuously for a long time without needing to be replaced and recharged periodically. In connection with the scale of power generation, micro-scale power well-designed has some advantages, i.e. more flexible, more efficient, more reliable related in diverse power input, higher energy density, higher power density, lower to zero emissions, lower noise pollution, lower maintenance, longer lifetimes,



wide range of applications, easier to control, no interrupts if integrated into the system, allowing for combined as the hybrid power generation [3, 4].

Microfluidic fuel cells as a novel technology that can be miniaturized and having a higher energy density than traditional membrane fuel cells and conventional Li-battery. Fuel cells have a high energy density, performance can be longer at operating time span, and only depends on the size volume of the fuel storage. Conversely, the batteries have a shorter operating time span which needed recharging again and is determined by the dimension of the battery as energy storage. A novelty design and structure of microfluidic fuel cells, also known as membrane less micro fuel cells (MFCs) or laminar flow-based fuel cells (LFFCs). Membrane-less microfluidic fuel cells (MFCs) is a miniaturized fuel cell without needing a proton membrane. They use an electrolyte as a substitute of the membrane which used to exchange proton. Microfluidic fuel cells contain liquid fuel and oxidant that flowing side by side along the microchannel [5-9]. Microfluidic fuel cells utilize the drawback of diffusive and convective mixing fluid by applying laminar flow at low Reynold number separate the fuel and oxidant, also to eliminate polymer membrane used in traditional fuel cells. Fluid flows either flowing through, flowing over, flowing between a top and down along the anode and cathode electrode. In the channel cell and porous media, mixing of the species can be occurred only in the diffusion process. The performance by enhancing an efficiency of current air-breathing microfluidic fuel cells have been investigated [10-12].

The aims of this study are to investigate various effects on the performance of direct formic acid microfluidic fuel cells that breathe air as an oxidant. Three-dimensional numerical simulation is developed for a formic acid air-breathing microfluidic fuel cells with flow-over anode-cathode electrode. The present computational model simulation is validated towards the experimental study and others published data.

2. Numerical Model

2.1. Structural model, dimensions, and experiments

A model of T-AMFCs having the dimension design of micro channel is 1.5 mm x 25 mm in width multiply length. In addition, both anode and cathode electrode having a width and length of 0.6 mm and 20 mm, respectively, with an electrode spacing of 0.3 mm. An air-breathing microfluidic fuel cell having a 0.6 mm in width and 20 mm in length that is placed on cathode GDE down-side. In figure 1 illustrates the structural model of a T-shape AMFCs. The model formed by seven layers that are composed of a fuel channel, electrolyte channel, oxidant channel (air-breathing at cathode electrode), anode electrode reaction catalyst layer, anode porous electrode gas diffusion layer, cathode electrode reaction catalyst layer, cathode porous electrode gas diffusion layer. In detail, the microchannel having two inlets, both anode inlet as fuel (formic acid mixed with sulfuric acid) and cathode inlet are filled with sulfuric acid as a proton conductor. The air-breathing cathode is exposed to the ambient air supply as well as the oxidant and penetrate into the porous electrode in contact with the electrolyte solution to generate water at the end of the channel outlet.

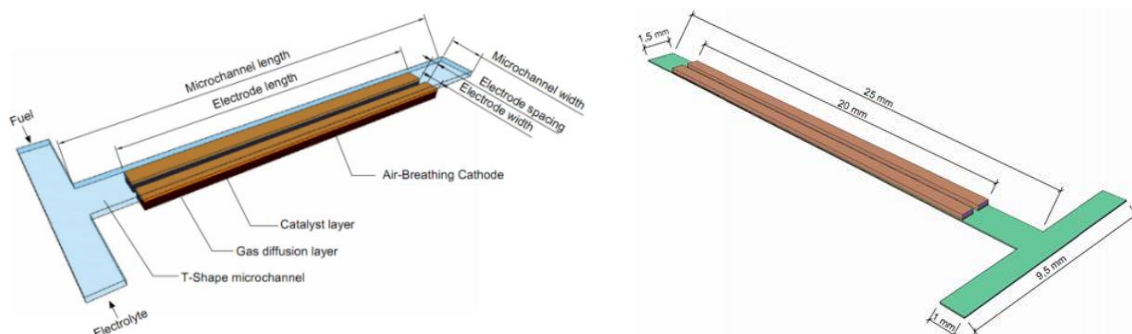


Figure 1. Schematic of the structural model T-shaped air-breathing direct formic acid fuel cells used in numerical simulation and the experimental study

A miniaturized fuel cell of the structure and design of a typical T-shaped air-breathing DFAFC shown in figure 1. In such systems for the fluid delivery, both formic acid (0.5 M) as a fuel solution mixing sulfuric acid (0.5 M) at a node channel side and as an electrolyte used sulfuric acid (0.5 M) place take on the cathode channel side are injected together into the end of the channel outlet by two syringe pumps. While sufficiency of the oxygen supply from the air is chosen as an oxidant. The electrolyte solution was added to both anode and cathode electrolyte channel to serve sufficiency proton ions, also the better proton conductivity at the electrochemical kinetic reactions. The anode and cathode porous electrode are deposited on the bottom side of a microchannel. In both the anolyte (fuel solution) and catholyte (electrolyte solution) stream takes place to contact and a reaction of the species so that proton ions produced at the anode side can transfer from the anolyte to the cathode electrode. In the air-breathing system, a stream of oxygen is exposed to the ambient air supply as well as the oxidant, and from cathode GDL bottom side penetrates into the porous electrode in contact with the electrolyte solution to generate water at the end of the channel outlet. The bottom surfaces of the anode and cathode electrode are electric ground and electric potential, respectively. They are as current collectors that generate an electronic conductivity connected to an electronic load circuit.

Table 1. Performance of direct formic acid fuel cell

Authors	Fuel/oxidant	Electrolyte	Current density (mA/cm ²)	Power density (mW/cm ²)	Channel size (mm)	Model features
Shaegh et al. [7]	HCOOH/air	H ₂ SO ₄	7.92	3.9	W x H x L 2.0 x 0.9 x 50	Air-breathing MFCs with a porous planar anode
Shaegh et al. [8]	HCOOH/air	H ₂ SO ₄	140	29	W x H x L 3.0 x 0.5 x 30	Air-breathing MFCs using fuel reservoir
Zhang et al. [5]	HCOOH/air	H ₂ SO ₄	117.6	13.2	W x H x L 2.0 x 3.0 x 44	Air-breathing MFCs with flow-over and flow-through anodes
Khabbazi et al. [6]	HCOOH/O ₂ + H ₂ SO ₄	H ₂ SO ₄	6	3.6	W x H x L 2.0 x 0.5 x 30	The effect of channel and electrode geometry
Jayashree et al. [14]	HCOOH/O ₂ + H ₂ SO ₄	H ₂ SO ₄	165	55	W x H x L 10 x 5.9 x 50	1G and 2G of Performance MFCs with flow-through anode
Zhu et al. [2]	HCOOH (1M)/air	H ₂ SO ₄	118.3	21.5	W x H x L 2.5 x 6.3 x 40	Air-breathing MFCs based on Cylinder electrodes
Shyu et al. [12]	HCOOH + H ₂ SO ₄ /air	H ₂ SO ₄	120	36	W x H x L 1.5 x 0.05 x 30	3G of Y-shape air-breathing MFCs with flow over the electrode

2.2. Boundary conditions

In this study, a numerical approach is performed based on domain system as shown in figure 1 was developed by COMSOL Multiphysics 5.1. While parameters constant and physical properties used in the model, including constant parameters, fluid properties, formic acid oxidation kinetics, and oxygen reduction kinetics, as shown in table 1. For simplification a three-dimensional numerical simulation analysis, some assumptions and boundary conditions are studied in the model development as follows:

- Fuel cell system is three-dimensional, steady-state, and isothermal domain;
- Flow fluid is laminar, incompressible, and continuity at all internal boundaries;
- Catalyst layers and GDLs are considered as an isotropic porous media and homogeneous;
- Electrochemical reactions take place on standard operating conditions at 25⁰ C, 1 atm;
- For Navier-Stokes equation, an initial velocity of fluid at the anode and the cathode channel inlet $(u, v, w) = (u_0, 0, 0)$, and $u_0 = 0.167$ m/s;
- Velocity for all channel walls is equal to zero, referred to as the no-slip conditions, $(u, v, w) = (0, 0, 0)$;
- Pressure channel outlet, $p = 0$, and an external force and gravity effect are neglected because of viscous dissipation at a low velocity;
- Pressure point constraint was employed in air-breathing boundary outlet, $p = 0$ at the end of the cathode electrode;

3. Results and Discussion

3.1. COMSOL model validation

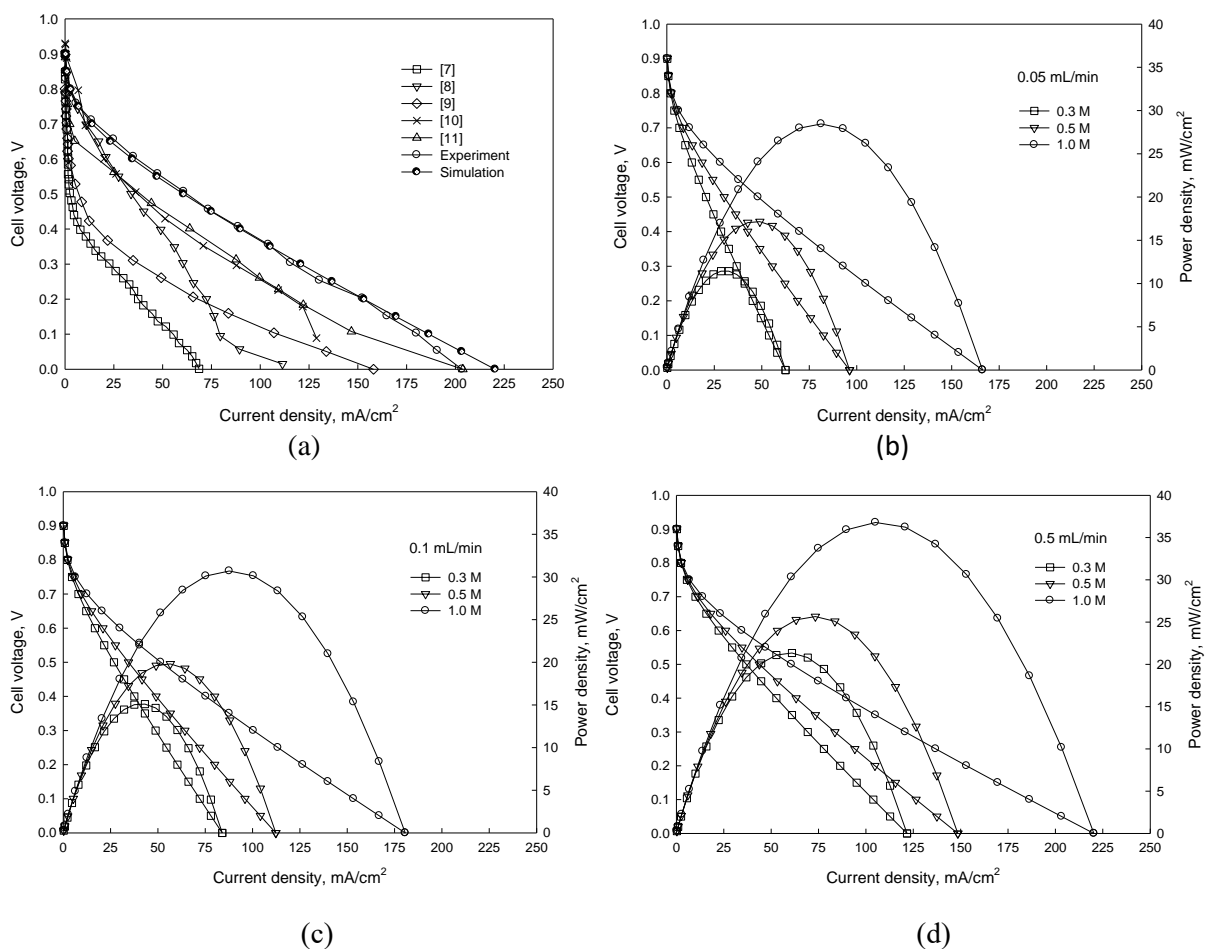


Figure 2. The overall performance air-breathing MFCs: (a) Performance comparison between the experimental vs simulation (1.0 M-HCOOH, 0.5 mL/min) and other published data; (b-d) V-I and P-I curves of the fuel cell operated at $[HCOOH] = 0.3$ M, 0.5 M, and 1.0 M with the volumetric flow rate of 0.05 mL/min, 0.1 mL/min and 0.5 mL/min

The following is a three-dimensional design display for generic drug packaging leak testing machines: In the numerical simulation value of the fuel cell as shown in Fig. 2(b-d), with a fuel concentration of 0.5 M, the maximum power density of the fuel cell was approximately 17.15 mW/cm², 19.81 mW/cm², and 25.65 mW/cm² at 0.05 mL/min, 0.1 mL/min, and 0.5 mL/min, respectively. The cell performance has a maximum power density of 36.78 mW/cm² at a current density of 105.1 mA/cm² at a fluid volumetric flow rate of 0.5 mL/min. The cell performance increases along with increasing fluid flow velocity of the microchannel cell. This will enhance fuel crossover at the cathode consequently, it will decrease a concentration of anolyte and catholyte stream.

The performance of I-V and power density curve are presented in figure 2 (a-d), respectively. Explicitly, the cell performance I-V and power density rise gradually in the concentration of fuel. Even though, the exchange current density on electrode of each curve in figure 2 (b-d) are not proportional to the concentration of fuel as well as the maximum power density in Fig. 2(b-d). As in the case of the cell performance for 0.5 M-HCOOH with volumetric flow rate of 0.5 mL/min in Fig. 2 (b-d), the cell current density on anode electrode increases from 96.27, 112.29, and 148.53 mA/cm², respectively, only as the fuel concentration increase from 0.3 M to 1 M-HCOOH at the proton conductivity of 16.7 S/m. In this case indicate that even though a stronger volumetric flow rate can enhance the transport of fuel to the anode electrode, this influence alleviates gradually and the concentration loss because of the inadequate transport of oxygen from ambient air into gas diffusion layer to the cathode electrode surface occurs lastly. In general, stronger volumetric flow rate and concentration will increase the cell performance, including the cell current density and the cell power density.

3.2. Fuel concentration distribution

The cell performance evaluated by a change of fuel concentration and oxygen concentration in the microchannel. Since the microfluidic fuel cell running on laminar flow, changes in the laminar flow velocity in the microchannel will effect of reactant transport and fuel cell performance. Depletion of fuel occurs at a high volumetric flow rate is replenished by the fuel stream rapidly. The fuel concentration profiles have the diffusion region becomes to change and moves to the channel outlet along with the volumetric flow rate increasing that will cause depletion fuel at the cathode channel outlet. The fuel losses at the channel outlet caused by mixed diffusion of different concentration and a high volumetric flow rate along with microchannel.

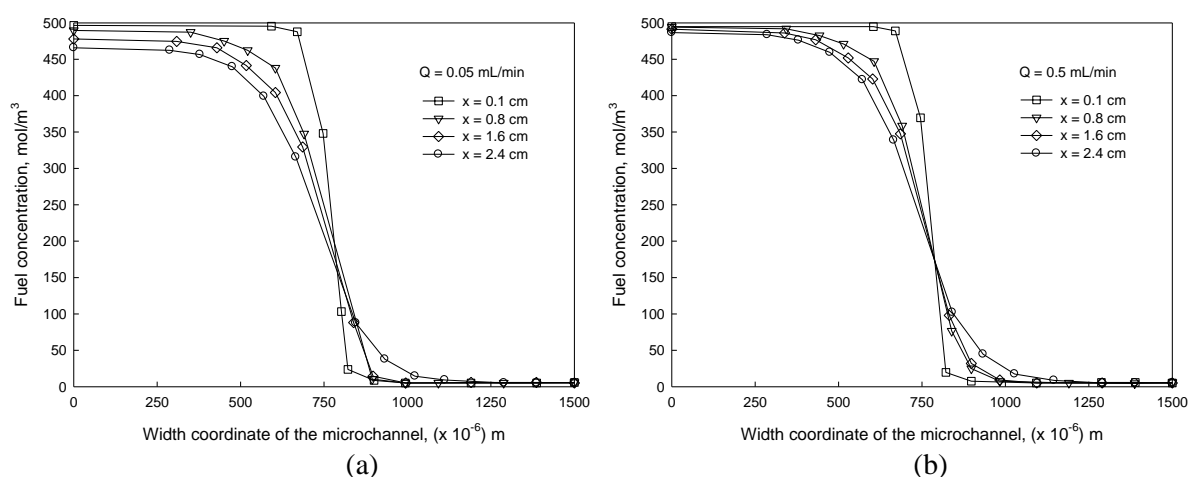


Figure 3. The formic acid concentration distribution along the microchannel at 4 specific positions of width coordinate of the channel with inlet [HCOOH] = 0.5 M on electrode surface of the microchannel: (a) flow rate of 0.05 mL/min; (b) flow rate of 0.5 mL/min

3.3. The local current distribution on the electrode surface

The current distribution generated on the electrode surfaces lower than the current distribution generated in the mid-plane along the channel due to the current that generated on the electrode surface closer to the catalyst layer in the electrochemical reaction process. The current density of the cathode electrode is negative, this matter corresponds to the oxidation reduction reaction where the electron leaves the cathode electrode move to the anode electrode. In this case, considering the cathode electrode has a negative overvoltage in which the actual voltage is lower than the reversible voltage, so the oxygen reduction reaction that dominates. In the operating fuel cell, the reduction of oxygen takes place of the cathode electrode. Moreover, the oxygen reduction of the cathode reaction needs a more significant overvoltage than the anode reaction.

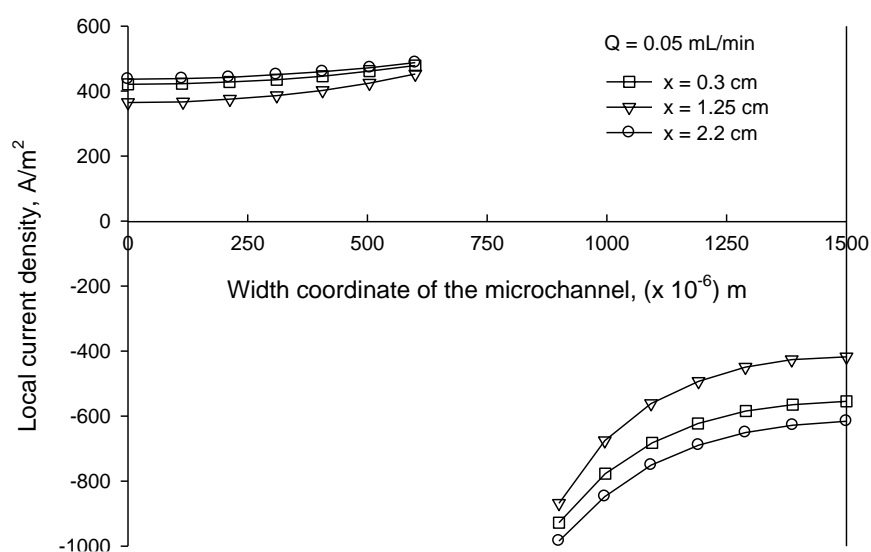


Figure 4. The local current distribution on electrode surface at 3 specific positions of width coordinate of the microchannel (x) with inlet $[\text{HCOOH}] = 0.5 \text{ M}$ at 0.05 mL/min

At low flow rates, a little number of fuel passing through the electrolyte and electron conduction through the electrolyte is known as fuel crossover. The current density decrease due to the concentration of fuel in anolyte stream decreases. The electrochemical oxidation reaction of fuel over the cathode can generate in a mixed voltage loss and drop the open circuit voltage. The performance of the local current density depends on the amount of the oxygen that transported to the catalyst layer. The current density distribution that affected by oxygen diffusion, seem uniform on the surface of the cathode catalyst. The local current density on the surface of the cathode catalyst layer is smaller than at the anode catalyst layer due to limitations of the diffusion that the reaction on the surface cannot be employed fully. The current distribution in the cathode catalyst layer reaches a maximum current as a function of the mass transport resistance, the ionic resistance, and charge transfer resistance. This means that the maximum current distribution in the cell is a function of the maximum depletion of the oxygen concentration in the outlet side of the channel and also the amount of the oxygen can be reacted and brought to the electrode surface of the mass transfer conditions. The increase current density corresponding with a decrease in oxygen concentration in the cathode catalyst layer. It seems that the local current density is almost uniformly shifted to the right side on the surface of the anode electrode. The local current density is low near the inlet, and gradually increases along the flow channel toward the channel middle, then decreases in the region near the outlet. The cell performance is higher in near the inlet region related to better electrolyte conductivity (lower ohmic overvoltage). The cell performance is lower in near the outlet because of higher the water flooding in

the cathode channel side. At a higher water content in the cathode catalyst layer the mass transport limitations in the gas diffusion layer will be reduced and conversely.

4. Conclusions

The results in this study represented measuring experiment and numerical simulation which performance HCOOH concentration of 0.5 M the maximum power density of the fuel at 0.5 0.6, 0.7 mL/min for experimental was approximately 31, 32.16, and 31 mW/cm², respectively, while the maximum power density of the fuel at 0.5 mL/min, for numerical simulation was approximately 21.34, 25.65, and 36.78 mW/cm², respectively. The result of the present study reveals that the cell open circuit potential slightly increased along with the increase of the fluid flow rate on the fuel reactant solution. The fuel mass transport pass through a microchannel above anode electrode is limited by species mass transfer and will enhance proton crossover in the cell. The major effects of proton/fuel crossover are a decrease of open circuit potential, and reduce the concentration of fuel above the anode electrode caused by mixing potential. In addition, that performance microfluidic fuel cells are affected by five factors, including electrolyte concentration, reactant concentration, microchannel geometry, fluid flow rate, electrode arrangement. This model presents concepts into the couple mass transport process and electrochemical reaction kinetics of an air-breathing microfluidic fuel cells, and can guidance future design and optimization. The local current density in the microfluidic fuel cells with different operating conditions of flow rate and concentration have experimentally measured and numerical simulation. The optimum cell performance occurs in the electrode region that have the most of the average distributed current density profiles. Further work in this field is the development and continued improvement of an air-breathing microfluidic fuel cell, including fuel utilization and power density in the near future to obtain the cell performance as a function all of the relevant parameters constant. In addition, in connection with the performance of fuel cells is necessary to develop a study of bubble formation inside the microchannel.

References

- [1] Kjeang E, Djilali N, and Sinton D, 2009 Microfluidic fuel cells: A review. *J. Pwr Sorcs.* 186 353-369.
- [2] Zhu Y, Ha S Y, and Masel R I, 2004 High power density direct formic acid fuel cells. *J. Pwr Sorcs* 130 8-14.
- [3] Jeong K J, Miese C M, Choi J H, Lee J, Han J, Yoon S P, Nam S W, Lim T H, and Lee T G, Fuel 2007 Crossover in direct formic acid fuel cells. *J. Pwr Sorcs.* 168 119-125.
- [4] Bazylak A, Sinton D, and Djilali N, 2005 Improved fuel utilization in microfluidic fuel cells: A computational study. *J. Pwr Sorcs.* 143 57-66.
- [5] Zhang B, Ye D D , Sui P C, Djilali N, and Zhu X, 2014 Computational modeling of air-breathing microfluidic fuel cells with flow-over and flow-through anodes. *J. Pwr Sorcs* 259 15-24.
- [6] Khabbazi A E, Richards A J, and Hoorfar M, 2010 Numerical study of the effect of the channel and electrode geometry on the performance of microfluidic fuel cells. *J. Pwr Sorcs.* 195 8141-8151.
- [7] Shaegh S A M, Nguyen N T, and Chan S H, 2010 An air-breathing microfluidic formic acid fuel cell with a porous planar anode: experimental and numerical investigations. *J. Mcromec and Mcroeng* 20 105008 12pp.
- [8] Shaegh S A M, Nguyen N T, Chan S H, and Zhou W, 2012 Air-breathing membrane less laminar flow-based fuel cell with flow-through anode. *J. Hydro En.* 37 3466-3476
- [9] Whipple, D T, Jayashree, R S, Egas, D, Vante, N A, Kenis, P J A. 2009 *Ruthenium cluster-like chalcogenide as a methanol tolerant cathode catalyst in air-breathing laminar flow fuel cells.* *Electrochim. Acta* 54 4384-4388.
- [10] Brushett F R, Jayashree R S, Zhou W P, and Kenis P J A, 2009 *Investigation of fuel and media flexible laminar flow-based fuel cells,* *Electrochimica Acta* 54 7099-7105.

- [11] Jayashree R.S, Yoon S K, Brushett F R, Lopez-Montesinos P O, Natarajan D, Markoski L J, and Kenis P J A, 2010 On the performance of membraneless laminar flow- based fuel cells, *J. Pwr. Sorcs.* 195 3569-3578.
- [12] Shyu J C, Wang P Y, Lee C L, Chang S C, Sheu TS, Kuo C H, Huang K L, and Yang Z Y, 2015 *Fabrication and test of an air-breathing microfluidic fuel cell*, *Energies* 8 2082-2096.
- [13] Shyu J C, Huang C L, Sheu T S, and Y H., 2012 *Experimental study of direct hydrogen peroxide microfluidic fuel cells*. *Micro and Nano Letters* 7 740-743
- [14] Jayashree R S, Gancs L, Choban E R, Primak A, Natarajan D L J, and Markoski, P J A, 2005 Keni, Air-Breathing Laminar Flow-Based Microfluidic Fuel Cell, *J. Amrcn. Chemic. Scity.* 127 16758-16759.

Acknowledgements

Y.D.H. would like to thanks to the Ministry of Research Technology and Higher Education of Indonesia for his research funding Penelitian Terapan Unggulan Perguruan Tinggi Tahun 2019.

Conflicts of Interest

The authors declare no conflict of interest.